Correlations between fission fragment yields and the prompt fission γ-ray spectrum

P. Jaffke[1], *P. Talou*[1], *T. Kawano*[1], *I. Stetcu*[1], *M. Devlin*[2], *N. Fotiades*[2], *C.-Y. Wu*[3], *and A. Chyzh*[3]
[1] Theoretical Division, Los Alamos National Lab, Los Alamos, NM 87545, USA
[2] Physics Division, Los Alamos National Lab, Los Alamos, NM 87545, USA
[3] Lawrence Livermore National Lab, Livermore, CA 94550, USA

Abstract
We illustrate correlations between the prompt fission γ-ray spectrum (PFGS) and the input fission fragment yields $Y(A)$ with a Monte Carlo implementation of the statistical Hauser-Feshbach decay theory, the `CGMF` code. We find that the slope of the PFGS at high γ-ray energies is correlated to the yields near the closed-shell ^{132}Sn nucleus. Low-energy PFGS peaks from discrete transitions of particular post-neutron fission products result from a complex interplay between the yields, the nuclear level structure, and the spin of nearby nuclei. We demonstrate this complexity with ^{128}Sn and derive level correction factors, which can be used to relate fission product yields to discrete transition intensities, for several even-even nuclei.

1 Introduction

The prompt γ-ray emission following nuclear fission is a resurging area of interest in the nuclear community for both experiment [1–3] and theory [4–6], due to its importance across a variety of applications. The prompt γ-ray contribution to the reactor heating [7] has been identified as a high-priority subject by the Nuclear Energy Agency [8]. In addition, the production of γ rays from isomers can provide an indirect probe of the spin of fission fragments [9]. Finally, γ-ray spectroscopy has been used to connect the fission product yields to the intensities of discrete γ-ray transitions [10, 11].

We utilize the `CGMF` code [4], a Monte Carlo implementation of the statistical Hauser-Feshbach theory [12], to model the prompt γ-ray and neutron emissions after fission. The code is described in full elsewhere [13], so we merely summarize the method here. Calculations begin by determining the initial distribution of fragments in mass A, charge Z, spin and parity J^{π}, and - indirectly - the excitation energy U. From this distribution, a pair of fragments, along with their J^{π} and U, are sampled. Each fragment is then sequentially decayed by the following process. Transition probabilities for neutron and γ-ray emissions are calculated using the global optical potential [14], strength-function formalism [15] with parameters from the RIPL-3 [16] database, and level densities from the Gilbert-Cameron formalism [17] supplemented with discrete levels from RIPL-3 [16]. Transition probabilities are then used to sample a neutron or γ-ray emission with a given energy. The process repeats with the residual nucleus until it decays to a stable or long-lived state, resulting in a list of all prompt neutrons and γ rays emitted for each fission event.

From the above method, one can see that the prompt fission γ-ray spectrum (PFGS) is a complicated calculation. To simplify this picture, we attempt to find correlations between PFGS properties and the input mass yields $Y(A)$. In particular, we correlate the slope of the PFGS at high γ-ray energies with the yields near the closed-shell ^{132}Sn nucleus. In addition, we discuss the complexities of discrete γ-ray transitions and calculate level corrections to relate the transition intensity to fission product yields.

2 PFGS high-energy slope

First, we test the impact of simple changes in the $Y(A)$ distribution on the PFGS using ^{239}Pu$(n_{\rm th}, f)$ as a case study. The pre-neutron mass distribution $Y(A)$ is often parameterized with 5 Gaussians, three of which are unique, as in Ref. [13]. On the left in Fig. 1, we display our fit to the experimental data [18–20] in red (solid), along with five other artificially shifted $Y(A)$. The fit captures the experimental trend

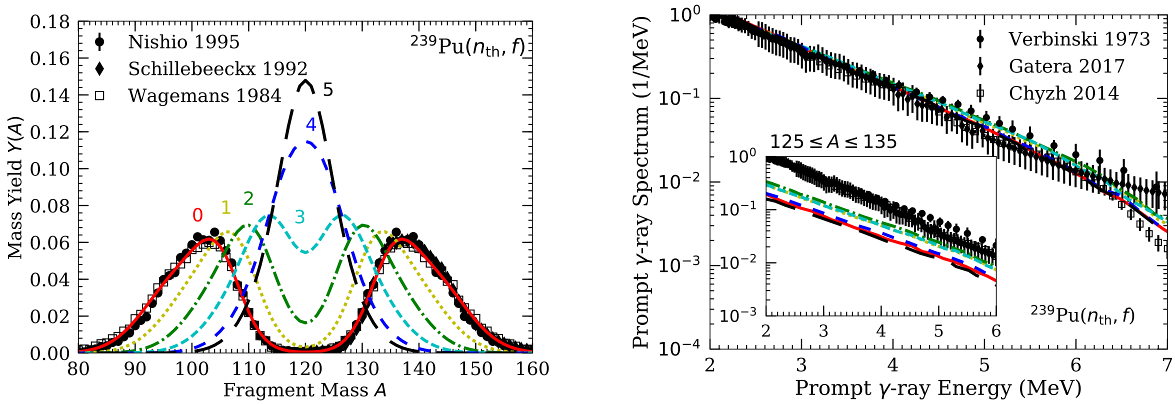

Fig. 1: Left: fitted pre-neutron mass yields $Y(A)$ from ^{239}Pu(n_{th}, f) to experimental data [18–20]. Exact fit is in solid red, with the other colors demonstrating an increasingly symmetric $Y(A)$. Right: resulting PFGS for the six input $Y(A)$ in 200 keV bins, alongside experimental data [1,2,21]. Insert shows the contribution from fission products with $125 \leq A \leq 135$, which drive the high-energy slope.

adequately and the shifts are determined by moving the Gaussian means towards symmetry. Thus, the red (solid) curve indicates the experimental result and the black (long dashed) is a fully symmetric yield, with the others in between.

Using the six different input $Y(A)$ shown on the left in Fig. 1, we perform six `CGMF` calculations, each with 500000 fission events. The resulting PFGS is plotted on the right in Fig. 1. We see that the slope of the PFGS is steeper for the red (solid), blue (medium dashed), and black (long dashed) calculations. This is because these $Y(A)$ had lower yields in the $125 \leq A \leq 135$ mass region, near doubly-magic ^{132}Sn. The level spacing of these products are known to be large [16], leading to higher energy γ-ray transitions. Thus, when a $Y(A)$ features these fragments more prominently, say in the yellow (dotted), green (dot-dashsed), and cyan (short dashed) cases, more high-energy γ rays are produced leading to a harder spectrum. The partial PFGS from the $125 \leq A \leq 135$ mass region is shown in the insert. The fitted slopes to the total PFGS are given in Tab. 1, where the slope changes by 9% between the $Y(A)$ following experimental ^{239}Pu(n_{th}, f) data to a fully symmetric $Y(A)$.

	$Y_0(A)$	$Y_1(A)$	$Y_2(A)$	$Y_3(A)$	$Y_4(A)$	$Y_5(A)$
Slope (1/MeV)	-0.243	-0.228	-0.222	-0.226	-0.236	-0.241
$125 \leq A \leq 135$ Contr.	18.7%	29.2%	33.8%	29.6%	21.0%	16.6%

Table 1: Fitted slopes to the $2-6$ MeV range of the PFGS for six input $Y(A)$ ranging from least to most symmetric (see text) and the PFGS contribution in this energy range from fission products with mass $125 \leq A \leq 135$.

3 Discrete transitions

Discrete transitions from fission products can manifest as low-energy peaks in the PFGS [2,21]. The peak intensity depends on the direct production of the fission product, but also on the probability that a given γ ray is emitted. This probability is a complex interplay between the initial spin distribution of the product and the level structure. To analyze this, three spin cases were calculated (each with 500000 events) for ^{238}U$(n = 1.75\,\mathrm{MeV}, f)$ using `CGMF`. The spin cases had an average spin over all fragments of $\langle J \rangle = 8.22, 9.94, 11.8\,\hbar$, which were chosen to span a reasonable range of prompt γ-ray multiplicities:

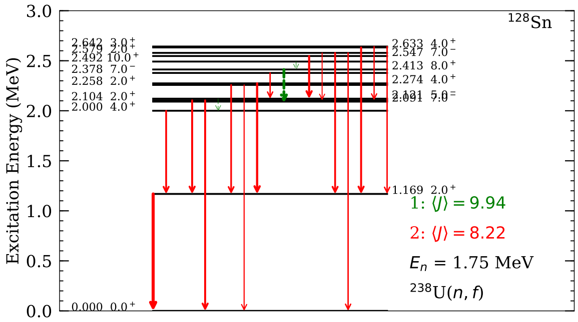

Fig. 2: Example emission scheme for ^{128}Sn produced in ^{238}U$(n = 1.75\,\mathrm{MeV}, f)$ fission. The arrows indicate transitions, where the colors (dashing) indicate which of two spin cases, $\langle J\rangle = 8.22\,\hbar$ (red solid) or $\langle J\rangle = 9.94\,\hbar$ (green dashed), had a larger transition probability. The thickness of the arrow indicates the magnitude of this probability difference. We note that ^{128}Sn has a $2.091\,\mathrm{MeV}$ isomer with a halflife of $6.5\,\mathrm{s}$.

$\bar{\nu}_\gamma = 7.4, 8.4, 9.5$ γ/fission. Larger $\langle J\rangle$ leads to higher γ-ray multiplicities as the nuclei emit more γ rays (typically E1 transitions in the continuum) to remove the excess spin, as shown in Ref. [22].

For each spin case, the transition scheme of specific fission products was analyzed. In Fig. 2, we plot the comparison of the ^{128}Sn emission scheme for $\langle J\rangle = 8.22\,\hbar$ (red, solid) and $\langle J\rangle = 9.94\,\hbar$ (green, dashed). Normalizing by the number of events producing ^{128}Sn, we compared the probability to emit 18 discrete transitions in each spin case. Transitions are colored according to which spin case showed a higher probability for a given transition. The arrow size corresponds to the magnitude of the probability difference between the two spin cases. For example, the $10^+ \rightarrow 8^+$ and $7^- \rightarrow 7^-$ transitions are more probable in the high-spin case, hence they are colored green in Fig. 2. However, the ground-state band $2^+ \rightarrow 0^+$ transition is red and large, suggesting it heavily favors low-spin cases. This is caused by the $6.5\,\mathrm{s}$ isomer at $U = 2.091\,\mathrm{MeV}$, which acts as a roadblock for subsequent transitions.

From the above discussion, it is clear that corrections, which can be estimated [23], must be used to relate the fission product yields to the intensity of γ-ray transitions. However, these corrections will depend on the spin distribution of the product and the timing window as well. We determine the corrections associated with the nuclear level structure using `CGMF` via

$$\eta(A_p, Z_p, \epsilon_\gamma) = \frac{Y(\epsilon_\gamma; A_p, Z_p)}{Y(A_p, Z_p)}, \tag{1}$$

where the probability to generate the product with mass A_p and charge Z_p after prompt neutron emission is $Y(A_p, Z_p)$. The probability to emit a γ ray of energy ϵ_γ *and* the product (A_p,Z_p) is $Y(\epsilon_\gamma; A_p, Z_p)$.

Figure 3 shows level correction factors for the ground-state band $2^+ \rightarrow 0^+$ transition of 19 even-even fission products using Eq. 1 and `CGMF`. The different curves correspond to the different spin cases. We note that the assumption that the ground-state band $2^+ \rightarrow 0^+$ transition is emitted every time the specified product is generated in fission would correspond to unity. These level corrections, as well as corrections for the use of a multiplicity cut, energy resolution, and timing window, are critical factors in γ-ray spectroscopy.

Overall, we find that the majority of studied $2^+ \rightarrow 0^+$ transitions would require corrections on the order of $10 - 20\%$ when correlating the fission product yields to the intensity of discrete γ-ray lines. Some nuclei, ^{128,132}Sn and ^{150}Ce, had much more severe corrections, primarily due to long-lived isomers and sparse level spacings. The derived correction factors depend on the discrete level data [16], as `CGMF` cannot predict level information. Thus, the calculation is only as reliable as the input data. We note that each fission reaction is unique, so the level corrections presented here are only applicable to ^{238}U$(n = 1.75\,\mathrm{MeV}, f)$. However, this process demonstrates that `CGMF` could determine similar level corrections for other fission reactions, allowing for more accurate results from γ-ray spectroscopic

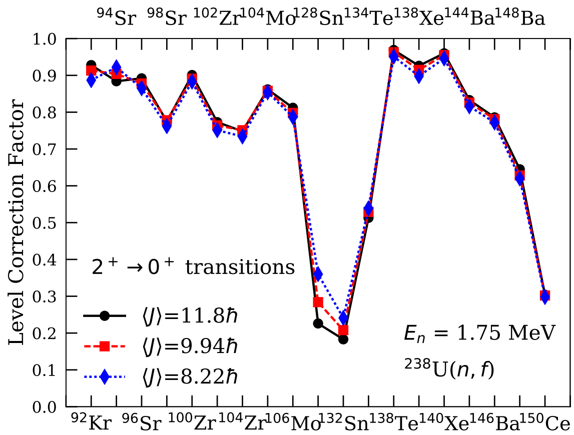

Fig. 3: Level correction factors (see text), which represent the percent of fission events producing the specified product and the ground-state band $2^+ \to 0^+$ transition, for 19 even-even fission products. Calculation for three spin cases of $^{238}\mathrm{U}(n = 1.75\,\mathrm{MeV}, f)$ are shown.

studies. In particular, we intend to demonstrate how these corrections and data from γ-ray detector arrays [24–26] could help infer fission product yields in a future work. This process has already been applied in Ref. [11] to provide a possible cause for some of the discrepancies observed in $^{238}\mathrm{U}(n, f)$ yields [10].

4 Summary

We have used a Monte Carlo Hauser-Feshbach model, CGMF, to simulate fission events and draw connections between the fission yields and the prompt fission γ-ray spectrum (PFGS). Focusing on the high-energy part of the PFGS, we found that the slope between $2-6\,\mathrm{MeV}$ is correlated with the production of fission products near doubly-magic ^{132}Sn, where the level spacing and, hence, average γ-ray energies are larger. After analyzing the low-energy discrete peaks in the PFGS, we found that the peak intensities are a complex interplay between the fission yields, the nuclear level structure, and the spin distribution. This was illustrated in the specific case of $^{238}\mathrm{U}(E_n = 1.75\,\mathrm{MeV}, f)$ and we proceeded to determine the level corrections for a variety of even-even fission products, over a range of spin cases. These corrections show that particular fission products are susceptible to large errors if their nuclear level structures are not accounted for properly. Therefore, it may be necessary to incorporate spin-dependent calculations of the level corrections into γ-ray spectroscopy studies of fission product yields.

Acknowledgements

This work was performed under the auspices of the US Department of Energy by Lawrence Livermore National Security, LLC under contract DE-AC52-07NA27344 and by Los Alamos National Security, LLC under contract DE-AC52-06NA25396. Partial funding is gratefully acknowledged from the U.S. DOE/NNSA Office of Defense Nuclear Nonproliferation Research and Development.

References

[1] A. Chyzh, C. Y. Wu, E. Kwan, R. A. Henderson, T. A. Bredeweg, R. C. Haight, A. C. Hayes-Sterbenz, H. Y. Lee, J. M. O'Donnell, J. L. Ullmann, Phys. Rev. C 90 (2014) 014602. doi:10.1103/PhysRevC.90.014602.

[2] A. Gatera, T. Belgya, W. Geerts, A. Göök, F.-J. Hambsch, M. Lebois, B. Maróti, A. Moens, A. Oberstedt, S. Oberstedt, F. Postelt, L. Qi, L. Szentmiklósi, G. Sibbens, D. Vanleeuw, M. Vidali, F. Zeiser, Phys. Rev. C 95 (2017) 064609. doi:10.1103/PhysRevC.95.064609.

[3] A. Chyzh, P. Jaffke, C. Wu, R. Henderson, P. Talou, I. Stetcu, J. Henderson, M. Buckner, S. Sheets, R. Hughes, B. Wang, J. Ullmann, S. Mosby, T. Bredeweg, A. Hayes-Sterbenz, J. O'Donnell, Physics Letters B 782 (2018) 652 – 656. doi:https://doi.org/10.1016/j.physletb.2018.06.006.

[4] B. Becker, P. Talou, T. Kawano, Y. Danon, I. Stetcu, Phys. Rev. C 87 (2013) 014617. doi:10.1103/PhysRevC.87.014617.

[5] O. Litaize, O. Serot, L. Berge, The European Physical Journal A 51 (12) (2015) 177. doi:10.1140/epja/i2015-15177-9.

[6] P. Talou, T. Kawano, I. Stetcu, J. P. Lestone, E. McKigney, M. B. Chadwick, Phys. Rev. C 94 (2016) 064613. doi:10.1103/PhysRevC.94.064613.

[7] G. Rimpault, D. Bernard, D. Blanchet, C. Vaglio-Gaudard, S. Ravaux, A. Santamarina, Physics Procedia 31 (2012) 3 – 12, gAMMA-1 Emission of Prompt Gamma-Rays in Fission and Related Topics. doi:https://doi.org/10.1016/j.phpro.2012.04.002.

[8] Nuclear data high priority request list of the nea (req. id: H.3, h4), http://www.oecd-nea.org/dbdata/hprl/hprlview.pl?ID=421 (2006).

[9] I. Stetcu, P. Talou, T. Kawano, M. Jandel, Phys. Rev. C 88 (2013) 044603. doi:10.1103/PhysRevC.88.044603.

[10] Wilson, J. N. and Lebois, M. and Qi, L. and Amador-Celdran, P. and Bleuel, D. and Briz, J. A. and Carroll, R. and Catford, W. and De Witte, H. and Doherty, D. T. and Eloirdi, R. and Georgiev, G. and Gottardo, A. and Goasduff, A. and Hadyńska-Klęk, K. and Hauschild, K. and Hess, H. and Ingeberg, V. and Konstantinopoulos, T. and Ljungvall, J. and Lopez-Martens, A. and Lorusso, G. and Lozeva, R. and Lutter, R. and Marini, P. and Matea, I. and Materna, T. and Mathieu, L. and Oberstedt, A. and Oberstedt, S. and Panebianco, S. and Podolyák, Zs. and Porta, A. and Regan, P. H. and Reiter, P. and Rezynkina, K. and Rose, S. J. and Sahin, E. and Seidlitz, M. and Serot, O. and Shearman, R. and Siebeck, B. and Siem, S. and Smith, A. G. and Tveten, G. M. and Verney, D. and Warr, N. and Zeiser, F. and Zielinska, M., Phys. Rev. Lett. 118 22 (2017) 222501. doi:10.1103/PhysRevLett.118.222501.

[11] N. Fotiades, P. Casoli, P. Jaffke, M. Devlin, R. Nelson, T. Granier, P. Talou, T. Ethvignot, submitted to Phys.Rev.C (2018).

[12] W. Hauser, H. Feshbach, Phys. Rev. 87 (1952) 366–373. doi:10.1103/PhysRev.87.366.

[13] P. Jaffke, P. Möller, P. Talou, A. J. Sierk, Phys. Rev. C 97 (2018) 034608. doi:10.1103/PhysRevC.97.034608.

[14] A. Koning, J. Delaroche, Nuclear Physics A 713 (3) (2003) 231 – 310. doi:https://doi.org/10.1016/S0375-9474(02)01321-0.

[15] J. Kopecky, M. Uhl, Phys. Rev. C 41 (1990) 1941–1955. doi:10.1103/PhysRevC.41.1941.

[16] R. Capote, M. Herman, P. Obložinský, P. Young, S. Goriely, T. Belgya, A. Ignatyuk, A. Koning, S. Hilaire, V. Plujko, M. Avrigeanu, O. Bersillon, M. Chadwick, T. Fukahori, Z. Ge, Y. Han, S. Kailas, J. Kopecky, V. Maslov, G. Reffo, M. Sin, E. Soukhovitskii, P. Talou, Nuclear Data Sheets 110 (12) (2009) 3107 – 3214, special Issue on Nuclear Reaction Data. doi:https://doi.org/10.1016/j.nds.2009.10.004.

[17] A. Gilbert, A. G. W. Cameron, Canadian Journal of Physics 43 (8) (1965) 1446–1496. arXiv:https://doi.org/10.1139/p65-139, doi:10.1139/p65-139.

[18] C. Wagemans, E. Allaert, A. Deruytter, R. Barthélémy, P. Schillebeeckx, Phys. Rev. C 30 (1984) 218–223. doi:10.1103/PhysRevC.30.218.

[19] P. Schillebeeckx, C. Wagemans, A. Deruytter, R. Barthélémy, Nuclear Physics A 545 (3) (1992) 623 – 645. doi:https://doi.org/10.1016/0375-9474(92)90296-V.

[20] K. Nishio, Y. Nakagome, I. Kanno, I. Kimura, Journal of Nuclear Science and Technology 32 (5) (1995) 404–414. arXiv:https://doi.org/10.1080/18811248.1995.9731725,

doi:10.1080/18811248.1995.9731725.

[21] V. V. Verbinski, H. Weber, R. E. Sund, Phys. Rev. C 7 (1973) 1173–1185. doi:10.1103/PhysRevC.7.1173.

[22] I. Stetcu, P. Talou, T. Kawano, M. Jandel, Phys. Rev. C 90 (2014) 024617. doi:10.1103/PhysRevC.90.024617.

[23] P. Casoli, Etude de la production de fragments dans la fission induite par neutrons sur l'uranium-238, Ph.D. thesis, Université de Bordeaux (2003).

[24] I.-Y. Lee, Nuclear Physics A 520 (1990) c641 – c655. doi:https://doi.org/10.1016/0375-9474(90)91181-P.

[25] W. Urban, J. Durell, W. Phillips, A. Smith, M. Jones, I. Ahmad, A. Barnett, M. Bentaleb, S. Dorning, M. Leddy, E. Lubkiewicz, L. Morss, T. Rzaca-Urban, R. Sareen, N. Schulz, B. Varley, Zeitschrift für Physik A Hadrons and Nuclei 358 (2) (1997) 145–151. doi:10.1007/s002180050291.

[26] W. Younes, J. A. Becker, L. A. Bernstein, P. E. Garrett, C. A. McGrath, D. P. McNabb, G. D. Johns, R. O. Nelson, W. S. Wilburn, AIP Conference Proceedings 529 (1) (2000) 192–199. arXiv:https://aip.scitation.org/doi/pdf/10.1063/1.1361378, doi:10.1063/1.1361378.